Photocurrent spectroscopy of $Zn_{1-x}Cd_xSe/ZnSe$ quantum wells in *p-i-n* heterostructures

R. Cingolani, M. Di Dio,* M. Lomascolo,* R. Rinaldi,† P. Prete, and L. Vasanelli
Dipartimento di Scienza dei Materiali, Università di Lecce, Via Arnesano, I-73100 Lecce, Italy

L. Vanzetti, F. Bassani,‡ A. Bonanni, L. Sorba,§ and A. Franciosi‖
Laboratorio Tecnologie Avanzate Superfici e Catilisi del Consorzio Interuniversitario di Fisica della Materia, Area di Ricerca di Trieste, Padriciano 99, I-34012 Trieste, Italy
and Department of Chemical Engineering and Materials Science, University of Minnesota, Minneapolis, Minnesota 55455
(Received 18 April 1994)

Photocurrent-spectroscopy studies were performed in the $10 < T < 300$ K temperature range on *p-i-n* heterostructures grown by molecular-beam epitaxy and incorporating $Zn_{1-x}Cd_xSe/ZnSe$ multiple quantum wells (with $x = 0.10$ and 0.25) in the undoped region. The extremely well-resolved excitonic features and corresponding continuum edges allowed us to obtain directly the exciton binding energies and compare the spectra with excitonic transition energies calculated taking into account the effect of strain.

Phototransport effects have been widely used to study the electronic properties of bulk semiconductors as well as semiconductor interfaces.[1-3] In particular, the photovoltage (PV) process generally involves the separation of photoexcited electrons and holes by band bending near a surface or junction. In an open circuit configuration, this results in a photovoltage that tends to reduce the built-in potential. When the circuit is closed on a suitable load resistor, a photocurrent will result. The magnitude of the signal will generally depend on the optical-absorption probability, on the carrier recombination velocity, and—in the presence of a photocurrent—on the resistance of the bulk material or junction, and therefore on temperature.

Application of phototransport techniques to the determination of electronic parameter in wide-gap, II-VI semiconductor materials and related multiple-quantum-well (MQW) structures has been attempted recently,[4,5] and met with only moderate success. These materials, and especially $Zn_{1-x}Cd_xSe/ZnSe$ MQW's, are attracting intense attention in connection with the development of coherent emitters operating in the blue and blue-green regions of the visible spectrum,[6-10] but still exhibit substantial problems as far as doping and contact fabrication are concerned. Also, only relatively limited information is available about the excitonic versus free-carrier nature of the optical processes involved in lasing, and, in general, about the excitonic parameters of these materials.[6-10] During PV measurements at room temperature on $Zn_{0.82}Cd_{0.18}Se/ZnSe$ MQW laser structures[4] and MQW *p-i-n* modulators,[5] heavy-hole exciton absorption features with $n = 1$ (E_{1HH}) were directly observed, while broader absorption features were tentatively assigned to $n = 1$ light-hole transitions (E_{1LH}), yielding an estimated excitonic binding energy of 36 meV, and a light-hole–heavy-hole splitting of some 56 meV in the 7.5-nm-thick ternary quantum wells.

In this work we report well-resolved photocurrent spectra of $Zn_{1-x}Cd_xSe/ZnSe$ MQW's (with $x = 0.10$ and 0.25) as a function of temperature. The MQW's were embedded in the undoped region of suitable *p-i-n* heterostructures. At variance with previous attempts to exploit PV techniques on this class of materials, we fabricated the *p* and *n* sides of the junction using epitaxially grown, highly doped *p*-type GaAs and *n*-type ZnSe layers, in order to reduce the problem of fabricating ohmic contacts to *p*-type ZnSe. All materials were grown by solid source molecular-beam epitaxy (MBE) on GaAs(001) wafers, following the methodology described in Refs. 11 and 12.

The layer sequence is schematically illustrated in the inset of Fig. 1. Beryllium-doped, 0.5-μm-thick, GaAs buffer layers ($p \sim 0.1-1.0\times10^{18}$ cm^{-3}) grown at 580 °C provided the *p*-type layers of the *p-i-n* heterostructures. The undoped regions of the junctions[13] were fabricated by growing 0.5-μm-thick ZnSe buffer layers at 290 °C, followed by ten-period $Zn_{1-x}Cd_xSe/ZnSe$ MQW's with $x = 0.10$ (sample *A*) or 0.25 (sample *B*). Each period was comprised of a 2.8-nm-thick ternary well, and a 21.7-nm-thick ZnSe barrier. The MQW's were grown at 250 °C with a 30-s growth interruption at each interface. The topmost *n*-type regions of the heterostructures were Cl-doped ($n \sim 10^{18}$ cm^{-3}), 0.5-μm-thick, ZnSe layers fabricated while slowly raising the temperature from 250 to 290 °C.

The heterostructures were prepared for the measurements by evaporating metallic contacts on both surfaces. Indium was used for the bottommost *p*-doped GaAs contact, whereas Au was deposited on the topmost *n*-type ZnSe layer. The contacts were approximately 100 nm thick, and the contact area was approximately 0.8 mm^2 in size. The *p-i-n* diodes were evaluated by means of current-voltage (*I-V*) measurements. Typical *I-V* curves at a temperature of 300 K are shown in Fig. 1, and compared well with the best results in the literature on the same type of materials.[6,7]

Photocurrent measurements were performed by mounting the sample on the cold finger of a closed-cycle He cryostat, equipped with an electronic temperature controller. Thin gold wires were attached by means of a silver-loaded conductive epoxy to the metallic contacts on the sample surfaces. We used a frontally mounted, tungsten halogen lamp monochromatized by a 1-m single grating monochromator to illuminate the sample through a suitable chopper. The typical power density at the sam-

ple surface was of the order of a few $\mu W\,cm^{-2}$, for a slit width of 100 μm. Under these conditions, the spectral resolution was better than 0.2 meV. The resulting photocurrent was detected as a function of photon energy by means of a lock-in amplifier (input impedance ~ 1 MΩ) and digitally stored.

Photocurrent spectra at different temperatures are displayed in Figs. 2 and 3 for samples *A* and *B*, respectively. A rich excitonic absorption structure is emphasized at low temperature for both types of samples. In the high-photon-energy range, the abrupt increase in photocurrent reflects optical absorption in the topmost *n*-type ZnSe layer, with a clear excitonic resonance near 2.81 eV. At energies lower than the band-gap edge of the ZnSe barriers, the photocurrent signal appears to reproduce in detail the expected joint density of states of the $Zn_{1-x}Cd_xSe$/ZnSe MQW's. In particular, sharp heavy-hole (HH) and light-hole (LH) excitonic features with corresponding well-defined continuum edges can be resolved. Fabry-Pérot oscillations (not shown) could also be observed in the transparency region of the heterostructure, because of the high quality of surfaces and interfaces.

The similarity of the measured photocurrent spectra to the expected optical absorption line shape of the *p-i-n* heterostructure is evidenced in Figs. 2 and 3. The dashed curves represent the absorption spectra recorded from the same samples after removing the substrate by selective chemical etching. Actually, this similarity depends on the choice of suitable geometric parameters for the heterostructures. Light absorption in the transparency region of the ZnSe barrier is absorbed in the $Zn_{1-x}Cd_xSe$/ZnSe quantum wells to produce electron hole pairs which are readily separated by the built-in potential gradient. In this case the current of minority carriers flowing across the junction is a drift current (I_{dr}). Assuming a photogeneration rate $G(x) = G_0 \alpha e^{-\alpha x}$, where α is the absorption coefficient, the drift current is

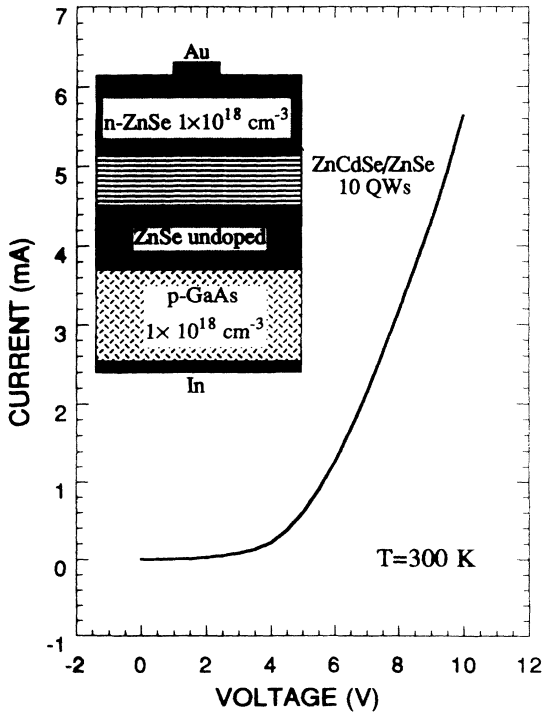

FIG. 1. Typical current-voltage characteristic of the investigated *p-i-n* heterojunctions at 300 K. The structure of the samples is depicted in the inset.

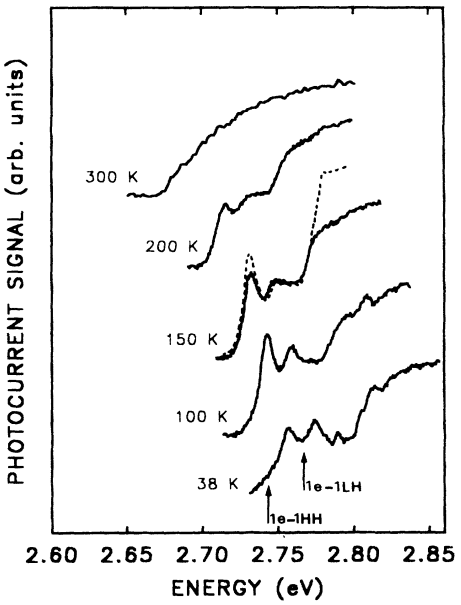

FIG. 2. Photocurrent spectra of sample *A* at different temperatures. The photocurrent curves have been multiplied by (-1) to evidence the similarity with the absorption spectra. Maxima in the spectra correspond to minimum photocurrent signal (i.e., strong absorption). The vertical arrows indicate the calculated excitonic transitions (see Table I). The dashed line is the absorption spectrum measured from the sample after selective chemical etching of the substrate.

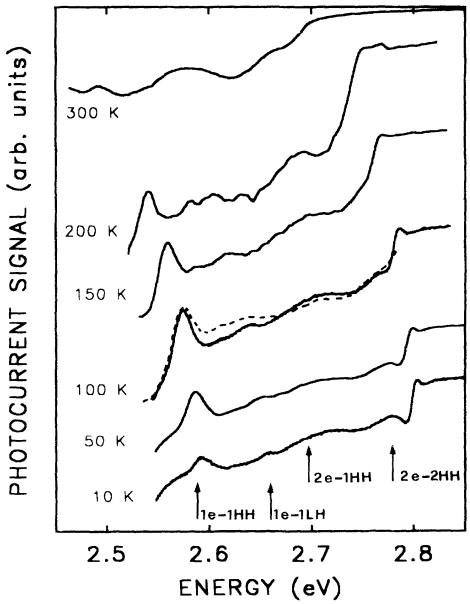

FIG. 3. Same as in Fig. 2 for sample *B*.

given by

$$I_{\rm dr} \cong q \int_0^W G(x)dx = qG_0(1-e^{-\alpha W}) \sim qG_0\alpha W \ , \quad (1)$$

where W is the thickness of the intrinsic region where absorption occurs. In the last term of Eq. (1) the exponential power expansion has been truncated to the first order ($\alpha W < 1$ in our samples). The implication is that to the first order the photocurrent signal is proportional to the absorption coefficient, but the departure from this proportionality may occur when the thickness of the intrinsic region W is too small, and the contribution of the diffusion current across the depletion layer has to be taken into account. This should introduce an additional dependence—generally nonlinear—of the photocurrent signal on the absorption coefficient, which would complicate the interpretation of the spectral line shape.

When optical absorption takes place outside the depletion layer, the detected photocurrent also depends strongly on the choice of suitable geometric parameters. For example, photons of energy $h\nu > 2.8$ eV are absorbed directly in the topmost ZnSe n-type layer, and in this case the photocurrent is primarily due to minority-carrier diffusion ($I_{\rm diff}$) from the top layer to the intrinsic region, provided that the top layer thickness is small enough—comparable to the carrier diffusion length—and large enough to minimize the opposite contribution due to the surface recombination velocity. A detailed analysis of the relationships between absorption and photocurrent spectra is presently underway in our laboratories, and will be the subject of a forthcoming paper.

The temperature dependence of the photocurrent spectra of the shallower quantum wells (Fig. 2, sample A, with 10% Cd content), shows that the light-hole exciton is ionized above 150 K, indicating a rather weak confinement. The heavy-hole exciton, on the other hand, seems more stable. Its binding energy, as deduced from the splitting between the exciton peak and the continuum edge in Fig. 2, is about 20 meV. This is consistent with the observed ionization of the HH resonance at a temperature of about 200 K. At room temperature the absorption profile becomes broad and featureless, reproducing the joint density of states of the bulk ZnSe topmost layer with a low-energy tail in the quantum-well region.

The deeper quantum wells (Fig. 3, sample B, with 25% Cd content) should give stronger excitonic confinement, by virtue of the stronger band-gap discontinuity. Indeed, the binding energy of the heavy-hole exciton deduced from the spectra amounts to about 36 meV. In this case the HH excitonic feature persists up to room temperature, whereas the LH band can still be observed above 200 K,[4,5] as can be seen in Fig. 3. Furthermore, distinct absorption structures are observed at higher energy in the quantum-well region (around 2.72 and 2.79 eV at 10 K), that we ascribe to the 2e-1HH transition (probably favored by the internal electric field) and the $n=2$ (2e-2HH) excitonic absorption, respectively. Such features are not observed for sample A, in which the $n=2$ electron and hole states are not confined in the shallow quantum well.

In order to quantitatively interpret the photocurrent spectra of Figs. 2 and 3, we have calculated the eigenstates of the quantum wells by means of the envelope-function method, within the effective-mass approximation. The strain effect was computed according to the Pikus and Bir Hamiltonian,[14] the heavy-hole and light-hole valence-band shifts being given by the following equations:

$$\Delta E_{\rm HH} = -2\alpha_v \left[\frac{C_{11}-C_{12}}{C_{11}}\right]\varepsilon + \beta\left[\frac{C_{11}+2C_{12}}{C_{11}}\right]\varepsilon \ , \quad (2)$$

$$\Delta E_{\rm LH} = -2\alpha_v \left[\frac{C_{11}-C_{12}}{C_{11}}\right]\varepsilon - \beta\left[\frac{C_{11}+2C_{12}}{C_{11}}\right]\varepsilon - 2\left[\beta\left[\frac{C_{11}+2C_{12}}{C_{11}}\right]\varepsilon\right]^2 \frac{1}{\Delta}\cdots \ , \quad (3)$$

where the elastic stiffness constants C_{ij}, the deformation potentials α and β ($\alpha_v = 1/3\alpha$), and the spin-orbit splitting Δ were taken from Ref. 15. The calculated compressive strain ε in the ternary wells amounts to 0.0072 for sample A and 0.018 for sample B. The lattice mismatch results in a reduction of the effective light-hole band discontinuity, thus causing shallower LH levels in the quantum well. On the other hand, the HH states are only weakly affected by the strain. Assuming a 80:20 conduction- to valence-band offset, and the effective masses reported in Ref. 16, we calculated the band discontinuities and the confinement energies listed in Table I.[17] Taking into account the heavy-hole exciton binding energies determined directly from the exciton–continuum-energy separation, we obtained the excitonic transition energies indicated by the vertical arrows in Fig. 1 and 2. The agreement between theory and

TABLE I. Electronic parameters calculated for the investigated samples (all numbers are in meV, except the Cd content). $\Delta E_{\rm HH,LH}$ are the strain-induced shifts of the electron–heavy-hole (HH) and electron–light-hole (LH) band edges of $Zn_{1-x}Cd_xSe$. $\Delta V_{e,\rm HH,LH}$ indicate the actual potential discontinuities experienced by the electrons (e), the heavy holes (HH), and light holes (LH) after having taken into account the strain. The quantization energies of the individual particles are labeled by E_j ($j=e$, HH, and LH). Note that the deepest quantum-well sample has the $n=2$ electron and the $n=2$ heavy-hole states confined in the well. E_b are the well exciton binding energies.

Sample	Cd content	$\Delta E_{\rm HH}$	$\Delta E_{\rm LH}$	ΔV_e	$\Delta V_{\rm HH}$	$\Delta V_{\rm LH}$	E_{1e}	$E_{1\rm HH}$	$E_{1\rm LH}$	E_{2e}	E_{2H}
A	10%	0.36	36	93.5	38.8	3.3	54	19	3		
B	25%	0.54	80.4	226.3	33.6	14.5	88	29	13	210	88

experiment is very good.

As deduced from the temperature-dependent photocurrent spectra of Figs. 2 and 3, the LH subbands are only weakly confined, being only a few meV below the band edge of the ZnSe barrier (see Table I). This is consistent with the observed disappearance of the LH exciton occurring in the photocurrent spectra above 150 K. Furthermore, the $n=2$ electron subband in sample B is resonant with the continuum of the conduction band. The related resonance in the spectrum appears like a broad band centered at the expected energy.

Finally, we emphasize that the presence of a well resolved ZnSe-related excitonic feature in the spectra of Figs. 2 and 3 allows us to evaluate directly the overall depth of the quantum well, i.e., the band-gap discontinuity. This is given by

$$\Delta E_g = E_g(\mathrm{ZnSe}) - E_g(\mathrm{Zn}_{1-x}\mathrm{Cd}_x\mathrm{Se}) = E_g(\mathrm{ZnSe}) - E_x + E_{1\mathrm{HH}} + E_{1e} , \quad (4)$$

where E_x is the measured exciton energy. The difference of the binding energies of the excitons in the ZnSe and in the quantum well can be neglected. The resulting values, which are only weakly dependent on the choice of the band offsets, reproduce fairly well those expected from the reported values of the ternary alloy band gap $E_g(\mathrm{Zn}_{1-x}\mathrm{Cd}_x\mathrm{Se})$ as a function of Cd content.[16,18]

The expert technical help of Donato Cannoletta is gratefully acknowledged. This work was supported in part by the U.S. Army Research Office under Grant No. DAAH04-93-G-0206, and by the Center for Interfacial Engineering of the University of Minnesota under NSF Grant No. CDR8721551.

*Permanent address: Centro Nazionale Ricerca e Sviluppo dei Materiali, Strada Statale 7, km 714.3, 72100 Brindisi, Italy.

†Permanent address: Dipartimento di Fisica, Università di Bari, Bari, Italy.

‡Present address: CRMC2-CNRS, Marseille, France.

§Also with Istituto ICMAT del CNR, Montelibretti, Roma, Italy.

‖Also with Dipartimento di Fisica, Università di Trieste, Trieste, Italy.

[1]See, for example, L. J. Brillson, in *Handbook on Semiconductors,* 2nd ed., edited by P. T. Landsberg (Elsevier, Amsterdam, 1992), Vol 1, Chap. 8.

[2]M. H. Heckt, Phys. Rev. B **41**, 7918 (1990); J. Vac. Sci. Technol. B **8**, 1018 (1990).

[3]X. Yu, A. Raisanen, G. Haugstad, G. Ceccone, N. Troullier, and A. Franciosi, Phys. Rev. B **42**, 1872 (1990).

[4]S. Y. Wang, J. Simpson, H. Stewart, S. J. A. Adams, I. Hauksson, Y. Kawakami, M. R. Taghizedeh, K. A. Prior, and B. C. Cavenett, Physica B **185**, 508 (1993).

[5]Y. Kawakami, S. Y. Wang, J. Simpson, I. Hauksson, S. J. A. Adams, H. Stewart, B. C. Cavenett, and K. A. Prior, Physica B **185**, 496 (1993).

[6]W. Xie, D. C. Grillo, R. L. Gunshor, M. Kobayashi, G. C. Hua, N. Otsuka, H. Jeon, J. Ding, and A. V. Nurmikko, Appl. Phys. Lett. **60**, 463 (1992).

[7]J. Qiu, H. Cheng, J. M. DePuydt, and M. A. Haase, J. Cryst. Growth **127**, 279 (1993).

[8]N. Peleknos, H. Haase, N. Magnea, H. Mariette, and A. Wasiela, Appl. Phys. Lett. **61**, 3154 (1992); N. T. Pelakanos, J. Ding, M. Hagerott, A. V. Nurmikko, H. Luo, N. Samarth, and J. K. Furdyna, Phys. Rev. B **45**, 6037 (1992).

[9]J. Ding, N. T. Pelekanos, J. Ding, A. V. Nurmikko, H. Luo, N. Samarth, and J. K. Furdyna, Appl. Phys. Lett. **57**, 2885 (1990).

[10]R. Cingolani, R. Rinaldi, L. Calcagnile, P. Prete, P. Sciacovelli, L. Tapfer, L. Vanzetti, Guido Mula, F. Bassani, L. Sorba, and A. Franciosi, Phys. Rev. B **49**, 16 769 (1994).

[11]G. Bratina, L. Vanzetti, R. Nicolini, L. Sorba, X. Yu, A. Franciosi, Guido Mula, and A. Mura, Physica B **185**, 557 (1993).

[12]L. Sorba, G. Bratina, A. Antonini, A. Franciosi, L. Tapfer, A. Migliori, and P. Merli, Phys. Rev. B **46**, 6834 (1992).

[13]The background doping for nominally undoped ZnSe and $\mathrm{Zn}_{1-x}\mathrm{Cd}_x\mathrm{Se}$ was estimated from Hall and resistivity measurements as $n \sim 1.5\times10^{15}$ cm^{-3}.

[14]H. Asai and K. Oe, J. Appl. Phys. **54**, 2052 (1983).

[15]*Numerical Data and Functional Relationship in Science and Technology,* edited by K. H. Hellwege, Landolt-Börnstein, New Series, Group III, Vol. 17, Pt. a (Springer-Verlag, Berlin, 1982).

[16]H. J. Lozykowski and V. K. Shastri, J. Appl. Phys. **69**, 3235 (1991).

[17]The offset used in this work seems to fit the optical data quite well. However, the actual value may change depending on the effective masses used in the calculations. A more precise determination of the electronic properties of these II-VI heterostructures is probably necessary for an accurate evaluation of the offset from the optical spectra.

[18]M. C. Tamargo, M. J. S. P. Brasil, R. E. Nahory, R. J. Martin, A. L. Weaver, and H. L. Gilchrist, Semicond. Sci. Technol. **6**, A8 (1991).